

## Strong polaronic effects on rutile TiO<sub>2</sub> electronic band edges

Clas Persson and Antonio Ferreira da Silva

Citation: *Appl. Phys. Lett.* **86**, 231912 (2005); doi: 10.1063/1.1940739

View online: <http://dx.doi.org/10.1063/1.1940739>

View Table of Contents: <http://apl.aip.org/resource/1/APPLAB/v86/i23>

Published by the [American Institute of Physics](#).

---

### Additional information on *Appl. Phys. Lett.*

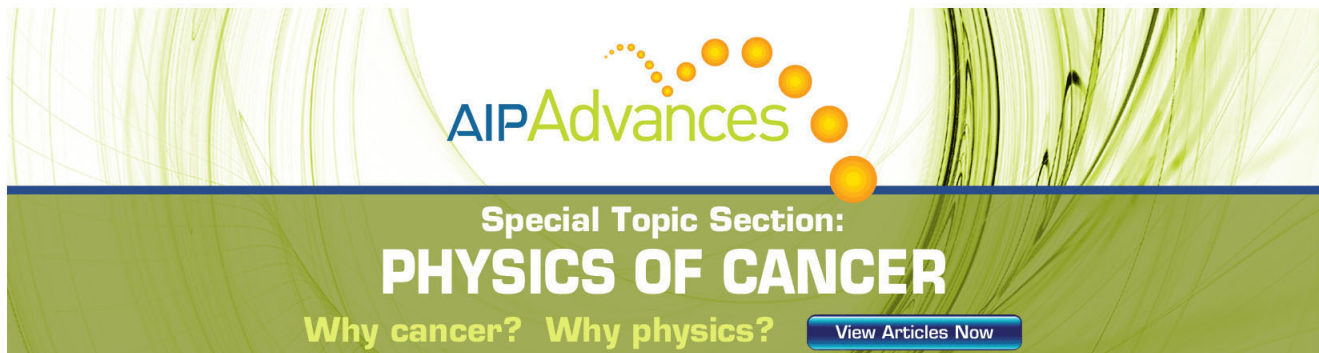
Journal Homepage: <http://apl.aip.org/>

Journal Information: [http://apl.aip.org/about/about\\_the\\_journal](http://apl.aip.org/about/about_the_journal)

Top downloads: [http://apl.aip.org/features/most\\_downloaded](http://apl.aip.org/features/most_downloaded)

Information for Authors: <http://apl.aip.org/authors>

## ADVERTISEMENT



AIPAdvances

Special Topic Section:  
**PHYSICS OF CANCER**

Why cancer? Why physics? [View Articles Now](#)

# Strong polaronic effects on rutile TiO<sub>2</sub> electronic band edges

Clas Persson<sup>a)</sup>

Applied Materials Physics, Department of Materials Science and Engineering,  
Royal Institute of Technology, SE-100 44 Stockholm, Sweden

Antonio Ferreira da Silva

Instituto de Fisica, Universidade Federal da Bahia, Campus Ondina, 40210-340 Salvador-BA, Brazil

(Received 29 December 2004; accepted 25 April 2005; published online 3 June 2005)

Thin TiO<sub>2</sub> films are prepared by dc magnetron sputtering as well as by the sol-gel technique, and the optical band edge absorption  $\alpha(\omega)$  is obtained from transmission spectroscopy. The electronic structure and optical properties are studied employing a first-principle linearized augmented plane-wave method within the local density approximation (LDA), improved by an on-site Coulomb self-interaction potential (LDA+ $U^{\text{SIC}}$ ). We show that the correction potential, the polaronic screening, and the spin-orbit interaction are crucial for determining the TiO<sub>2</sub> effective electron and hole masses. The dielectric function  $\varepsilon(\omega) = \varepsilon_1(\omega) + i\varepsilon_2(\omega)$  and the high-frequency constant  $\varepsilon(0 \ll \omega \ll E_g/\hbar)$  show pronounced anisotropy. The electron-optical phonon interaction affects  $\varepsilon(\omega \approx 0)$  strongly. © 2005 American Institute of Physics. [DOI: 10.1063/1.1940739]

The performance of low-scale TiO<sub>2</sub> based devices, such as dynamic random access memory and metal-oxide-semiconductor field effect transistor<sup>1</sup> is primarily determined by the electronic band edges of the materials,<sup>2,3</sup> i.e., the band energy location, dispersion, and symmetry of the conduction band (CB) and valence band (VB) edges. The effective electron  $m_c$  and hole  $m_v$  masses are used in various analyses and carrier transport simulations. Today, most theoretical studies of condensed matter rely on the local density approximation (LDA), which overall yields very good electronic structures. However, LDA underestimates the band gap energy  $E_g$  of semiconductors by  $\sim 30\text{--}60\%$ , and  $E_g(\text{LDA})=0$  with incorrect VB degeneracy for several important materials like Ge and InN. This band gap error  $\Delta_g(\text{LDA})$  is attributed to a missing discontinuity in the exchange-correlation potential and the LSD self-interaction error. It has recently been shown that LDA consistently fails to predict the  $\Gamma$ -point effective masses.<sup>4</sup> This is evident for GaAs where LDA yields  $m_c = 0.018m_0$ , which is significantly smaller than measured  $0.067m_0$ .<sup>5</sup> Thus, a proper correction to LDA is essential for predicting band edge physics of semiconductors.

In this letter, we study the electronic band edge structure of rutile ( $D_{4h}^{14}$ ) TiO<sub>2</sub> by means of a fully relativistic, full-potential linearized augmented plane-wave (FPLAPW) method,<sup>6</sup> using the LDA potential  $V(\text{LDA})$  in combination with a modeled on-site self-interaction correction (SIC) potential.<sup>7</sup>

$$V_l(\text{LDA} + U^{\text{SIC}}) = V(\text{LDA}) + \frac{U_l}{2} \left( 1 - 2 \sum_{m,\sigma} n_{m,\sigma} \right), \quad (1)$$

where  $n_{m,\sigma}$  is the occupancy of the  $l$  orbitals. We show that this LDA+ $U^{\text{SIC}}$  approach is suitable for studying the band-edge properties of TiO<sub>2</sub>. We find that the optical phonon screening affects strongly both the electron and hole masses. This electron-optical phonon coupling has also strong influence on the optical properties, here represented by the static

$\varepsilon(0)$  and high-frequency  $\varepsilon(\infty) \equiv \varepsilon_1(0 \ll \omega \ll E_g/\hbar)$  limits of the dielectric function  $\varepsilon(\omega) = \varepsilon_1(\omega) + i\varepsilon_2(\omega)$ . The FPLAPW optical absorption coefficient  $\alpha(\omega)$  is compared with measured transmission spectra of thin TiO<sub>2</sub> films, prepared by dc magnetron sputtering<sup>8</sup> as well as by sol-gel.<sup>9</sup> The transmission spectroscopy uses a halogen lamp as light source, and the polychromatic beam is diffracted by plane gratings. A first order bandpass filter has been used to avoid second order contamination. The energy gap resolution is  $\sim 2.8\%$ .

LDA underestimates localization of  $d$  states,<sup>10</sup> and as a consequence, the LDA cation-anion  $3d2p$  hybridization in ZnO disagrees with soft x-ray emission spectra.<sup>11</sup> This incorrect LDA hybridization was corrected within LDA+ $U^{\text{SIC}}$  using  $U_d(\text{Zn}) = 6$  eV.<sup>11</sup> Our calculated LDA band gap energy of rutile TiO<sub>2</sub> is  $E_g(\text{LDA}) = 1.8$  eV. The LDA+ $U^{\text{SIC}}$  band gap  $E_g(\text{LDA} + U^{\text{SIC}}) = 2.97$  eV using  $U_d(\text{Ti}) = 10$  eV fits to the low-temperature absorption data  $E_g = 3.0$  eV by Pascualet al.<sup>12</sup> The FPLAPW/LDA+ $U^{\text{SIC}}$  electronic structure [Fig. 1(a)] reveals a CB minimum consisting of two energetically close-lying bands; the energy difference is only 0.11 eV at the  $\Gamma$  point. These two CBs have rather flat energy dispersions, especially in the transverse ( $\perp$ ) direction. Higher lying CBs are 0.62–0.73 eV above the CB minimum at the  $\Gamma$  point. In the longitudinal ( $\parallel$ ) direction these bands

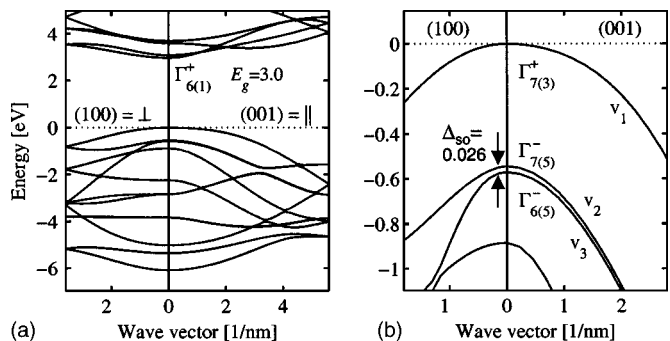


FIG. 1. (a) Electronic structure of rutile TiO<sub>2</sub>. (b) Close-up near the  $\Gamma$ -point VB maximum. Notation of irreducible representations  $\Gamma_{\alpha}^{\pm}$  is according to Ref. 13.

<sup>a)</sup>Electronic mail: clas.persson@kth.se

TABLE I.  $\Gamma$ -point band energies (in units of electron-volts and referred to VB maximum, cf. Fig. 1),  $\Gamma$ -point effective bare electron and hole masses (in units of  $m_0$ ), and corresponding polaron masses  $m^p$ . Spin-orbit interaction is included.

Band	$E_n(\Gamma)$	$m_{\perp}$	$m_{\perp}^p$	$m_{\parallel}$	$m_{\parallel}^p$
CBs					
$\Gamma_{7(4)}^+$	3.08	0.88	1.59	1.14	1.79
$\Gamma_{6(1)}^+$	2.97	1.41	2.52	0.60	0.97
VBs					
$\Gamma_{7(3)}^+$	0.00	1.74	4.53	2.98	6.38
$\Gamma_{7(5)}^-$	-0.54	0.54	0.82	0.94	1.33
$\Gamma_{6(5)}^-$	-0.57	0.54	0.82	0.94	1.33

are mixed with the two lowest CBs. Also the uppermost VBs have flat energy dispersions, and the second and third VBs are only 0.54 eV below the  $\Gamma$ -point VB maximum. The flat energy dispersions of these CBs and VBs favor a strong optical absorption. However, flat energy dispersion normally implies large conductive mass which affects the carrier lifetime.

The effective mass tensor  $m_n(\mathbf{k})$  of the  $n$ :th eigenstate  $E_n(\mathbf{k})$  is defined as  $1/m_n(\mathbf{k})_{ij} = \partial^2 E_n(\mathbf{k}) / \hbar^2 \partial k_i \partial k_j$ . Both effective electron and hole masses of rutile  $\text{TiO}_2$  evince strong anisotropic band curvatures (e.g.,  $m_{c1,\perp}/m_{c1,\parallel} = 2.35$ ; Table I). Moreover,  $m_{c1,\perp} = 1.41m_0$  ( $1.12m_0$ ) and  $m_{v1,\perp} = 2.98m_0$  ( $4.27m_0$ ) including (excluding) the SIC potential, and thus this correction is very important. It has been demonstrated<sup>13,14</sup> that the effective masses can strongly depend on the spin-orbit interaction even for light materials; the heavy-hole mass in 3C-SiC is reduced from  $15.0m_0$  to  $1.32m_0$ ,<sup>13</sup> and the  $\Gamma$ -point hole mass of zinc-blende AlN is negative unless spin-orbit interaction is included.<sup>14</sup> This effect is due to split of band degeneracy. In  $\text{TiO}_2$  the spin-orbit coupling affects mainly the second and third VBs due to the  $\Gamma_5^- \otimes D_{1/2} \Rightarrow \Gamma_6^- \oplus \Gamma_7^-$  split with  $\Delta_{\text{so}} = 26$  meV [Fig. 1(b)]. For instance,  $m_{v2,\perp} = 0.54m_0$  ( $0.94m_0$ ) and  $m_{v3} \approx m_{v2}$  ( $m_{v3} \ll m_{v2}$ ) including (excluding) the spin-orbit interaction, which is analogous to hexagonal SiC.<sup>13</sup>

Due to the ionic character of the Ti-O bonds, vibrations of the longitudinal optical (LO) phonons build up an electric field which screens the carries. This is described as a change in the effective masses. The resulting polaron mass  $m^p$  is here estimated from the energy  $\hbar\omega_{\text{LO}}$  of the long wavelength LO phonon and the dielectric constants, assuming nondegenerate bands, harmonic oscillation, and the effective mass approximation.<sup>15</sup>  $m^p = m / (1 - \alpha/6)$ , where  $\alpha = \sqrt{2me^4 \omega_{\text{LO}} \hbar^{-1} \cdot [\varepsilon(\infty)^{-1} - \varepsilon(0)^{-1}] / [8\pi\varepsilon(0)\hbar\omega_{\text{LO}}]}$  is the Fröhlich constant. We use the experimental neutron-scattering phonon frequency  $\hbar\omega_{\text{LO}} = 46$  meV by Traylor *et al.*<sup>16</sup> The polaronic effect in  $\text{TiO}_2$  is very large (e.g.,  $m_{v1,\perp}^p = 4.53m_0 \approx 2.5 \cdot m_{v1,\perp}$ , see Table I) which is due to the low LO phonon frequency and the large ration  $\varepsilon(0)/\varepsilon(\infty)$ . We suggest that the hopping transport in  $\text{TiO}_2\text{:Co}$  seen by Kennedy *et al.*<sup>17</sup> can partly be explained by local polaronic trapping.

The dielectric function  $\varepsilon(\omega)$  describes the electronic response to a change in the charge distribution, and the response is thus an important property for describing electronic screening near dopants, defects, and other structural perturbations.  $\varepsilon(\omega)$  is here calculated within the linear response theory from the joint density-of-states and the optical momentum matrix in the long wave length limit  $|\mathbf{k}' - \mathbf{k}| = 0$ :

$$\varepsilon_2^{ij}(\omega) = \frac{4\pi^2 e^2}{\Omega m_0^2 \omega^2} \sum_{\mathbf{k}, n, n', \sigma} \langle \mathbf{k}, n, \sigma | \hat{p}_i | \mathbf{k}, n', \sigma \rangle \times \langle \mathbf{k}, n', \sigma | \hat{p}_j | \mathbf{k}, n, \sigma \rangle f_{\mathbf{k}n\sigma} \cdot (1 - f_{\mathbf{k}n'\sigma}) \cdot \delta(E_{n'\sigma}(\mathbf{k}) - E_{n\sigma}(\mathbf{k}) - \hbar\omega) \quad (2a)$$

$$\varepsilon_1(\omega) = 1 + \frac{1}{2\pi} \int d\omega' \varepsilon_2(\omega') \left( \frac{1}{\omega' - \omega} + \frac{1}{\omega' + \omega} \right), \quad (2b)$$

where  $f_{\mathbf{k}n\sigma}$  is the Fermi distribution. The delta Dirac function indicates the importance of describing the band gap correctly. Electronic calculations exclude electron-phonon interactions, however, for polar materials  $\varepsilon(0)$  can only be determined by including this screening. We model the electron-optical phonon interactions with a delta-like absorption at the transverse phonon frequency  $\omega_{\text{TO}}$ :  $\varepsilon_2^{\text{ep}}(\omega) = \delta(\omega - \omega_{\text{TO}}) \pi \varepsilon_1(\infty) \cdot (\omega_{\text{LO}}^2 - \omega_{\text{TO}}^2) / 2\omega_{\text{TO}}$ . The imaginary part of the dielectric function [Fig. 2(a)] shows a small onset to absorption at 3.0–3.5 eV, associated with the direct transitions near the  $\Gamma$  point. The strong onset at  $\sim E_g + 0.5 = 3.5$  eV is due to absorption involving higher lying CBs and lower lying VBs (cf. Fig. 1). These bands are thus outmost important for band edge absorption in rutile  $\text{TiO}_2$ . At low photon energies, the effect due to the electron-phonon coupling is evident [inset in Fig. 2(b)]. The calculated static  $\varepsilon_{\perp}(0) = 144$ ;  $\varepsilon_{\parallel}(0) = 171$  and high-frequency  $\varepsilon_{\perp}(\infty) = 6.4$ ;  $\varepsilon_{\parallel}(\infty) = 7.4$  constants agree well with experimental results:  $\varepsilon_{\perp}(0) = 111$ ;  $\varepsilon_{\parallel}(0) = 257$  (see Ref. 18) and  $\varepsilon_{\perp}(\infty) = 6.8$ ;  $\varepsilon_{\parallel}(\infty) = 8.4$  (Ref. 16). Calculated  $\varepsilon_{\perp,\parallel}(0)$  depends strongly on variations in the electronic dispersion and in  $\hbar\omega_{\text{LO}}$ , which also are reflected by the strong measured temperature dependence<sup>18</sup> and growth dependence.<sup>19</sup> Theoretically,  $\varepsilon_{\perp,\parallel}(\infty)$  is obtained

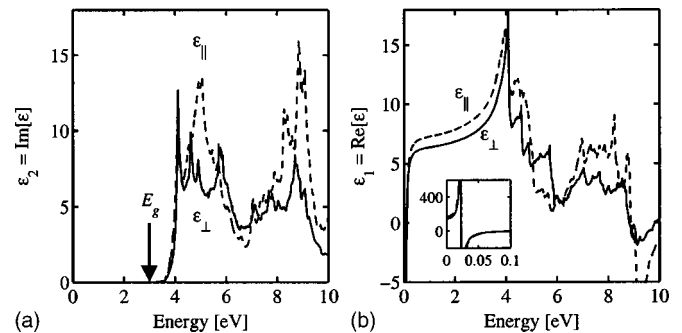


FIG. 2. Transverse ( $\perp$ ) and longitudinal ( $\parallel$ ) components of the (a) imaginary  $\varepsilon_2$  and (b) real  $\varepsilon_1$  parts of the dielectric function of rutile  $\text{TiO}_2$ . The inset shows (with same units as for the main figure) the strong effects on  $\varepsilon_1$  arising from absorption at  $\hbar\omega_{\text{TO}} = 26$  meV due to electron-phonon coupling.

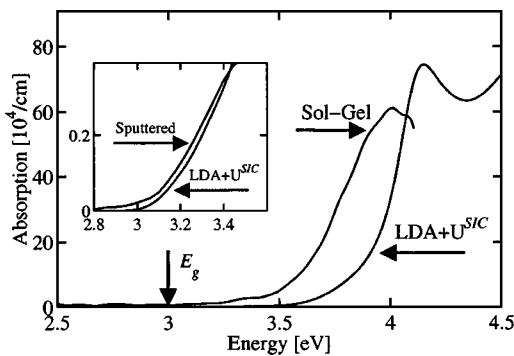


FIG. 3. Total absorption spectra of sputtering rutile and amorphous sol-gel  $\text{TiO}_2$ . The inset shows (with same units as for the main figure) the weak linear band edge absorption at 3.0–3.5 eV.

from  $\varepsilon_{\perp,\parallel}(\omega \rightarrow 0)$  excluding the electron-phonon coupling. This yields somewhat lower value compared to the experimental  $\varepsilon_{\perp,\parallel}(0 \ll \hbar\omega \ll E_g)$  value. Overall, the dielectric function of  $\text{TiO}_2$  shows strong anisotropy, and the large ratio  $\varepsilon(0)/\varepsilon(\infty) \approx 23$  demonstrates the importance of the electron-phonon coupling.

The absorption coefficient  $\alpha(\omega)$  is obtained from  $\varepsilon_1^2(\omega) + \varepsilon_2^2(\omega) = [\varepsilon_1(\omega) + \alpha^2(\omega)c^2/2\omega^2]$ . The LDA+ $U^{\text{SIC}}$  absorption coefficient and the transmission spectroscopy absorption spectrum of sputtered rutile  $\text{TiO}_2$  agree well (inset in Fig. 3), although the measured absorption is shifted slightly to lower photon energies, reflecting temperature effects. The absorption peak at 4.15 eV agrees with reflection measurements by Cardona and Harbeke.<sup>20</sup> The very weak absorption at 3.0–3.5 eV is a consequence of the symmetry-forbidden optical transitions  $\Gamma_{7(3)}^+ \rightarrow \Gamma_{6(1)}^+ \Gamma_{7(4)}^+$  at the  $\Gamma$ -point. Away from the  $\Gamma$ -point, transitions are allowed, but low since wave functions vary continuously. Thus, density-of-states cannot alone (i.e., without optical matrix elements) be used in analyses of optical properties of  $\text{TiO}_2$ . The weak linear band edge absorption allows identification of nonlinear optical absorption.<sup>21</sup> Amorphous  $\text{TiO}_2$  sol-gel films show absorption shifted  $\sim 0.2$ – $0.3$  eV towards lower energies (Fig. 3).

We conclude that the LDA+ $U^{\text{SIC}}$  potential describes the band edge properties of rutile  $\text{TiO}_2$  fairly accurately. The advantage of LDA+ $U^{\text{SIC}}$  is a computational time in the same order as LDA. The SIC correction, the polaronic screening, as well as the spin-orbit interaction are crucial for determining the effective masses. The total static

$[2\varepsilon_{\perp}(0) + \varepsilon_{\parallel}(0)]/3 = 153$  and high-frequency  $[2\varepsilon_{\perp}(\infty) + \varepsilon_{\parallel}(\infty)]/3 = 6.7$  dielectric constants agree well with measured  $\varepsilon(0) = 159.6$  (see Ref. 18) and  $\varepsilon(\infty) = 7.3$  (Ref. 16).

This work was financially supported by the Swedish Research Council (VR) and the Brazilian National Research Council (CNPq).

- <sup>1</sup>K. Kim, C. G. Hwang, and J. G. Lee, *IEEE Trans. Electron Devices* **45**, 598 (1998); S. A. Campbell, D. C. Gilmore, X.-C. Wang, M.-T. Hsieh, H.-S. Kim, W. L. Gladfelter, and J. Yan, *ibid.* **44**, 104 (1997).
- <sup>2</sup>G. Liu, T. Schulmeyer, A. Thissen, A. Klein, and W. Jaegermann, *Appl. Phys. Lett.* **82**, 2269 (2003); A. C. Tuan, T. C. Kaspar, T. Droubay, J. W. Rogers, Jr., and S. A. Chambers, *ibid.* **83**, 3734 (2003).
- <sup>3</sup>Z. J. Luo, X. Guo, T. P. Ma, and T. Tamagawa, *Appl. Phys. Lett.* **79**, 2803 (2001).
- <sup>4</sup>C. Persson and S. Mirbt, *Br. J. Phys.* (to be published).
- <sup>5</sup>N. E. Christensen, *Phys. Rev. B* **30**, 5753 (1984); C. Persson, R. Ahuja, and B. Johansson, *ibid.* **64**, 033201 (2001).
- <sup>6</sup>P. Blaha, K. Schwarz, G. K. H. Madsen, D. Kvasnicka, and J. Luitz, WIEN2k, an APW + local orbitals program for calculating crystal properties (K. Schwarz, Techn. Univ. Wien, Austria, 2001). Potential was obtained using  $\sim 1250$  plane waves and the modified tetrahedron  $\mathbf{k}$ -space integration with a  $\Gamma$ -centered mesh of 30  $\mathbf{k}$ -points in the irreducible part of the Brillouin zone. Optical properties were obtained with a 15 times larger  $\mathbf{k}$  mesh.
- <sup>7</sup>M. T. Czyzyk and G. A. Sawatzky, *Phys. Rev. B* **49**, 14211 (1994); V. I. Anisimov, I. V. Solovyev, M. A. Korotin, M. T. Czyzyk, and G. A. Sawatzky, *ibid.* **48**, 16929 (1993); A. I. Liechtenstein, V. I. Anisimov, and J. Zaanen, *ibid.* **52**, R5467 (1995).
- <sup>8</sup>T. Lindgren, J. M. Mwabora, E. Avendaño, J. Jonsson, A. Hoel, C.-G. Granqvist, and S.-E. Lindqvist, *J. Phys. Chem. B* **107**, 5709 (2003).
- <sup>9</sup>A. Conde-Gallardo, M. García-Rocha, I. Hernández-Calderón, and R. Palomino-Merino, *Appl. Phys. Lett.* **78**, 3436 (2001).
- <sup>10</sup>C. Persson and A. Zunger, *Phys. Rev. B* **68**, 073205 (2003).
- <sup>11</sup>C. L. Dong, C. Persson, L. Vayssieres, A. Augustsson, T. Schmitt, M. Mattesini, R. Ahuja, C. L. Chang, and J.-H. Guo, *Phys. Rev. B* **70**, 195325 (2004).
- <sup>12</sup>J. Pascual, J. Camassel, and H. Mathieu, *Phys. Rev. B* **18**, 5606 (1978).
- <sup>13</sup>C. Persson and U. Lindefelt, *J. Appl. Phys.* **82**, 5496 (1997).
- <sup>14</sup>C. Persson, A. Ferreira da Silva, R. Ahuja, and B. Johansson, *J. Cryst. Growth* **231**, 397 (2001).
- <sup>15</sup>*Polarons in Ionic Crystals and Polar Semiconductors*, edited by J. T. Devreese (North-Holland, Amsterdam, 1972).
- <sup>16</sup>J. G. Traylor, H. G. Smith, R. M. Nicklow, and M. K. Wilkinson, *Phys. Rev. B* **3**, 3457 (1971).
- <sup>17</sup>R. A. Parker, *Phys. Rev.* **124**, 1719 (1961).
- <sup>18</sup>R. J. Kennedy, P. A. Stampe, E. Hu, P. Xiong, S. von Molnár, and Y. Xin, *Appl. Phys. Lett.* **84**, 2832 (2004).
- <sup>19</sup>S. K. Kim, W.-D. Kim, K.-M. Kim, C. S. Hwang, and J. Jeong, *Appl. Phys. Lett.* **85**, 4112 (2004).
- <sup>20</sup>M. Cardona and G. Harbeke, *Phys. Rev.* **137**, A1467 (1965).
- <sup>21</sup>X. Zhu, Q. Li, N. Ming, and Z. Meng, *Appl. Phys. Lett.* **71**, 867 (1997).